

UC Davis

IDAV Publications

Title

Visualization Approaches to the Analysis and Display of Paleomagnetic Data

Permalink

<https://escholarship.org/uc/item/3ww2z3m9>

Author

Jurru, Elisabeth R.

Publication Date

1999

Peer reviewed

**Visualization Approaches to the Analysis and Display of Paleomagnetic
Data**

by

ELIZABETH R. JURRUS

B.S. (California Lutheran University) 1996

THESIS

Submitted in partial satisfaction of the requirements for the degree of
MASTERS OF SCIENCE

in

Computer Science

in the

OFFICE OF GRADUATE STUDIES

of the

UNIVERSITY OF CALIFORNIA

DAVIS

Approved:

Committee in Charge

1999

Abstract

Paleomagnetism is the study of the history of the geomagnetic field of the earth. Traditionally, paleomagnetists represent their three-dimensional data with two-dimensional plots. As the speed of sample collection and data analysis increases, there is a strong need to replace existing forms of analysis. By using visualization approaches, we have developed new ways to represent paleomagnetic data so that they can be studied with more efficiency and intuition by paleomagnetists. These new approaches increase the speed at which existing paleomagnetic data sets can be analyzed, provide a means of dealing with the very large data sets that are being generated by automated sampling handling systems, and create new methods for analyzing the data.

Acknowledgements

This work was supported by the National Science Foundation under contract DMS 95-10511, awarded to the University of California, Davis. I would like to thank J. Fritz Barnes and Eric LaMar and all the members of the Visualization Group at the Center for Image Processing and Integrated Computing at the University of California, Davis for their help. Very special thanks to Dr. Ken Joy for his guidance, patience, faith in me, and daily encouragement. I also want to thank Joseph Stoner and Adam Harris and all the members of the Paleomagnetism Laboratory, but especially Dr. Ken Verosub for his expert direction, teaching, and advice.

And lastly, I would like to thank Spatz and Mooches who let me spend long nights away from home at the laboratory.

Contents

1	Introduction	1
2	Collection and Analysis of Samples	6
3	Calculation of the Characteristic Natural Remanent Magnetization	9
3.1	Principal Component Analysis	10
3.2	NRM Visualization	14
4	Collective Data Analysis	19
4.1	Time-Sequence Analysis	20
4.2	Core Merging and Analysis	23
5	Virtual Geomagnetic Poles	25
5.1	Polarity Transitions	25
5.2	Paleosecular Variation on a Sphere	26
5.3	Paleosecular Variation Plotted with a Common Origin	28
6	Demagnetization Profiles	30
7	Conclusions	33
7.1	Implementation	34
	Bibliography	35

Chapter 1

Introduction

The earth is surrounded by a magnetic field which changes over time. Determining the behavior of the geomagnetic field and its spatial and temporal variations comprise one of the more established geophysical disciplines, paleomagnetism. Under appropriate circumstances, a record of the direction of the earth's magnetic field is preserved by geologic materials, such as rocks and sediments. Paleomagnetic methods can be used to recover this record and to establish its reliability. One use of this information is to determine the history of the magnetic field and to use this history to study the geochronology or tectonic movements of a particular geographic area.

The study of paleomagnetism begins with the collection and analysis of samples from appropriate earth materials. When sediment is deposited in a lake or ocean, when a lava flow cools at the surface of the earth, or when pottery is fired in a kiln, the magnetic grains of the material become magnetized parallel to the earth's magnetic field. Under favorable conditions, this magnetization can be preserved over geologically (or archaeologically)

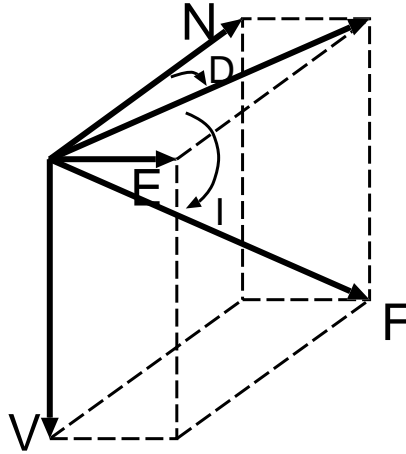


Figure 1.1: Magnetic Components declination (D) and inclination (I) and their relationship to east (E), north (N), and vertical (V).

significant periods of time. The goal of most paleomagnetic studies is the identification and isolation of the primary or original direction of magnetization of these materials (see [1]).

The geomagnetic field at a particular point can be represented by a vector. This vector has three components: inclination, declination, and intensity (see Figure 1.1). Inclination is the angle of the vector above or below the horizontal plane. Declination is the deviation of the horizontal component from true north, and intensity is the length of the vector. We can describe changes in the magnetic field by examining changes in intensity, declination, and inclination over time.

The traditional approach to the analysis of paleomagnetic data was developed for studies involving only a small number of samples. Today, as automated sample-handling systems and in-line demagnetization equipment become more common [11], the number of samples used in a typical paleomagnetic study is steadily growing. In many cases, the time required to analyze the data exceeds the time required to both collect the samples and make the measurements.

Another important trend is that until recently, the focus of most paleomagnetic

studies was the directional record of the geomagnetic field. Except for time-consuming studies that were specifically designed to determine the absolute paleointensity of the field, little attention was paid to the intensity of magnetization of individual samples. However, today there is more interest in the vector nature of the geomagnetic field than there has been since the inception of paleomagnetism almost fifty years ago. There is also evidence that changes in the directional record of the geomagnetic field are coupled to changes in the intensity record.

These developments make it more important to be able to analyze and display paleomagnetic data using automated three-dimensional techniques. We have developed a suite of six computer applications that implement three-dimensional visualization of the data, coupled with automated data analysis techniques:

- **Calculation of the characteristic natural remanent magnetization.** The traditional approach to the analysis of paleomagnetic data is to determine the characteristic directions of magnetization using *Zijderveld plots* [12], which date back to the earliest days of paleomagnetic research. We improve upon this approach by displaying the data in three dimensions, allowing the researcher to more accurately view the analysis. In addition, we implement an algorithm that determines the characteristic directions automatically.
- **Viewing a sequence of paleomagnetic directions.** In addition to improving the analysis of single samples, we have improved upon the analysis of data from large suites of samples. Once a suite of samples has been analyzed individually, it is important to be able to look at the changes in inclination, declination, and intensity down-core. With modern studies, this may involve data from 1000 samples or more. By viewing

the data sequence as a row of vectors along a spine, we can improve on the “old” method of two-dimensional analysis that shows only one component of the vector at a time.

- **Merging paleomagnetic data from several sediment cores to form a complete geomagnetic record.** Given data from several sediment cores, we want to merge the records or make comparisons between them. Previously, this was done in two dimensions by examining each component as a separate plot for each core and adjusting the data accordingly. We have improved upon this technique by comparing the cores in three dimensions. This allows viewing of all the components of each core at the same time. We are able to make adjustments to the data in real time by adjusting the declination and relative position of each core, thereby providing immediate feedback. After we have merged several cores together, we can produce a complete record of the magnetic field.
- **Virtual geomagnetic poles on a sphere.** Previously, viewing virtual geomagnetic poles (VGPs) meant projecting the appropriate data onto a plane and viewing several graphs for each data set. With three-dimensional techniques we can view the data on a sphere, eliminating the need for multiple plots.
- **Paleosecular variation plotted with a common origin.** Small-scale changes in the earth’s magnetic field are most often viewed as a projection onto a plane or as a two-dimensional *stereographic projection* with the intensity removed (see [1]). For this application, we present visualization techniques that extend this method and allow examination of the full three-dimensional vector. Here, we show directions as vectors anchored to a common origin creating a “movie” that shows the change of direction

and intensity over time.

- **Three-dimensional coercivity profiles.** We have also developed new techniques that allows us to view the magnetic properties of a large number of samples. Using a three-dimensional display of the intensity at each demagnetization level as a function of position along a sediment core, we can more quickly identify places where the magnetic coercivity is high or low. Before three-dimensional analysis techniques, there was no simple way of representing this data.

These new approaches have expanded on previous forms of analysis and have led to the development of new techniques for the analysis of the earth's magnetic field. This effort is the initial step toward the integration of visualization methods into the field of paleomagnetism.

Chapter 2

Collection and Analysis of Samples

Paleomagnetism studies begin with the collection of rock or sediment samples from the earth. There are two main forms of sample collection: Samples of rock are collected as oriented cores drilled in the field using a diamond-core drill; and sediments and soils are collected in small oriented plastic boxes or, more recently, in long plastic tubes called u-channels. Figure 2.1 shows a sediment core with small plastic boxes embedded in the sediment. The use of the u-channel, a long rectangular plastic channel, produces a long continuous sample which can be collected very quickly, since it takes less time to remove one long plastic tube than it does to remove many small plastic boxes.



Figure 2.1: Collection of samples from a core. Once the core has been retrieved, small plastic boxes are placed along the core to collect the sediment. Each box is also labeled to keep track of its relative position.



Figure 2.2: Long-core cryogenic magnetometer. A u-channel is placed on a track that automatically feeds the samples into the instrument for measurement.

The initial magnetization of a sample brought into the laboratory is known as the *natural remanent magnetization* (NRM). It represents the superposition of the original, or *characteristic* magnetization, with all of the various *secondary* magnetizations that the sample might have acquired. In order to recover the primary magnetization, the secondary magnetization is removed using one of several progressive demagnetization methods. These methods sequentially demagnetize a sample at successively higher levels, with measurements of the remaining NRM following each demagnetization.

The Paleomagnetism Laboratory at the University of California, Davis, currently uses two magnetometers to perform the measurement process. The older magnetometer, acquired by the lab in 1984, is used for plastic boxes and requires approximately one hour to step-wise demagnetize and measure each sample. The new long-core cryogenic magnetometer (Figure 2.2) uses u-channels and an automated sampling system that can in two hours do the same operations on 150 samples with very little operator intervention. This makes it possible to analyze samples seventy-five times faster than before.

The demagnetization process yields a sequence of paleomagnetic directions and intensities for each sample. The first few points of the sequence reflect the secondary magnetizations of the sample. But, as the demagnetization process continues, the characteristic NRM will appear. A principal component analysis, as described in the next section, is

usually used to determine the vector direction of the characteristic NRM.

Chapter 3

Calculation of the Characteristic Natural Remanent Magnetization

The first computer application involves calculation of the characteristic natural remanent magnetization (NRM). After a sample has been subjected to the demagnetization process, we use computational techniques to determine the characteristic NRM. A single measurement sequence contains approximately ten data points which represent the measured magnetization after each demagnetization step. By performing a principal component analysis (PCA) on a subset of these data points, we can determine the original direction, or characteristic NRM, of the magnetic field at the time of deposition. The difficult part lies in choosing which set of points we want to use for the PCA. This can be done two ways: the user is allowed to select which points to include or the computer chooses them automatically by evaluating all possible combinations of points. If the computer performs the automated analysis, it will select the subset of points that have the smallest maximum angular deviation (MAD). This indicates that our PCA fit, or regression line, lies as close

as possible to the selected set of points.

3.1 Principal Component Analysis

To do a principle component analysis, we use a set of n points in three-dimensional space. Let H be the 3×3 covariance matrix defined as

$$H = \begin{pmatrix} \sum (x_i)^2 & \sum (x_i y_i) & \sum (x_i z_i) \\ \sum (x_i y_i) & \sum (y_i)^2 & \sum (y_i z_i) \\ \sum (x_i z_i) & \sum (y_i z_i) & \sum (z_i)^2 \end{pmatrix}. \quad (3.1)$$

The matrix H can be transformed into $U^T L U$, where L is a diagonal matrix and U is orthonormal [3]. The diagonal elements of L are the eigenvalues λ_{\max} , λ_{mid} , and λ_{\min} of H (ordered by decreasing absolute value), and the columns of U contain the corresponding normalized eigenvectors \vec{e}_{\max} , \vec{e}_{mid} , and \vec{e}_{\min} . The eigenvalues are inversely related to the variance of these data in the direction of each eigenvector. These mutually perpendicular eigenvectors define the three axes of a local coordinate frame.

We can use the values of λ_{\max} , λ_{mid} , and λ_{\min} to understand the “shape” of the point set. Three cases are possible:

- Two eigenvalues – λ_{mid} and λ_{\min} – are zero, and one eigenvalue – λ_{\max} – has a finite, non-zero absolute value. This implies that the n points are collinear.
- One eigenvalue – λ_{\min} – is zero, and the other two eigenvalues – λ_{\max} and λ_{mid} – have finite, non-zero absolute values. This implies that the n points are coplanar.
- All three eigenvalues have finite, non-zero absolute values.

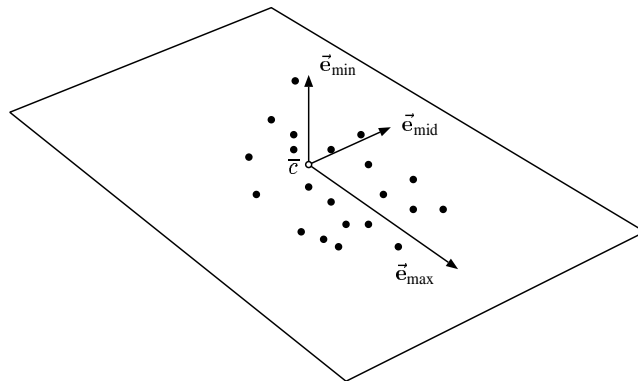


Figure 3.1: Principal component analysis (PCA) of a set of points in three-dimensional space. PCA yields three eigenvectors that form a local coordinate system about the origin, \bar{c} . The largest eigenvectors \vec{e}_{\max} defines a line that represents the best fit through the points. The eigenvectors, \vec{e}_{mid} and \vec{e}_{\min} , define a plane normal to that line.

The vector \vec{e}_{\max} defines the *orthogonal regression line*, which minimizes the sums of the squares of deviations perpendicular to the line itself. This vector represents the most accurate fit of a line to a set of points. The vectors \vec{e}_{mid} and \vec{e}_{\min} describe the regression plane which minimizes the sums of the squares of the deviations perpendicular to the plane. Figure 3.1 illustrates this local coordinate system.

The vector \vec{e}_{\max} represents the characteristic NRM. One way to measure the reliability of \vec{e}_{\max} is to examine the deviation of the data points from the vector direction. The maximum angle of deviation (MAD) is the largest calculated angle between the regression line and a line from the origin to each point in the sample. Figure 3.2 shows an example of this calculation.

Kirschvink [6] did not have high-performance computing systems at his disposal when he initially applied PCA to the analysis of paleomagnetic data. Instead of calculating the angle of deviation for each sample, he attempted to approximate the “maximum” deviation using the eigenvalues and eigenvectors calculated from the PCA.

Given eigenvalues λ_{\max} , λ_{mid} , and λ_{\min} , and corresponding eigenvectors \vec{e}_{\min} , \vec{e}_{mid} ,

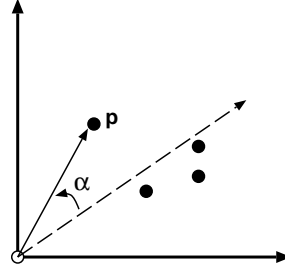


Figure 3.2: Maximum angular deviation (MAD) of a set of points. The angle, α , represents the largest angle from the regression line to any point. In this case p is the point that gives the MAD value.

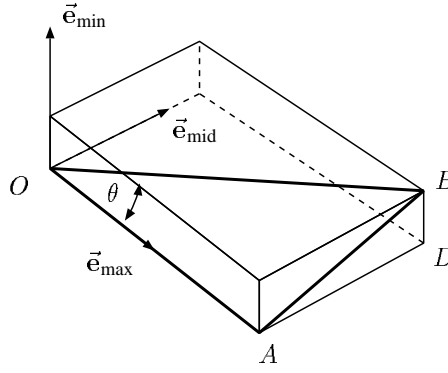


Figure 3.3: The angle AOB represents the MAD_1 value.

and \vec{e}_{\max} , the rectangular box aligned along the axes defined by the eigenvectors \vec{e}_{\min} , \vec{e}_{mid} and \vec{e}_{\max} , having sides of length $\sqrt{\lambda_{\min}}$, $\sqrt{\lambda_{\text{mid}}}$, and $\sqrt{\lambda_{\max}}$, defines the “standard deviation box” that surrounds the points and is proportional to the area generated by the data set. A first approximation to the maximum angular deviation of the samples is the angle θ shown in Figure 3.3. Here, the line \overline{OA} is the regression line and the angle θ represents the angle from the regression line to the farthest corner of the box (defined by line \overline{OB}).

The angle θ can be calculated directly by noting that the line \overline{OA} has length $\sqrt{\lambda_{\max}}$, the line \overline{AD} has length $\sqrt{\lambda_{\text{mid}}}$, and the line \overline{BD} has length $\sqrt{\lambda_{\min}}$. We can calculate the

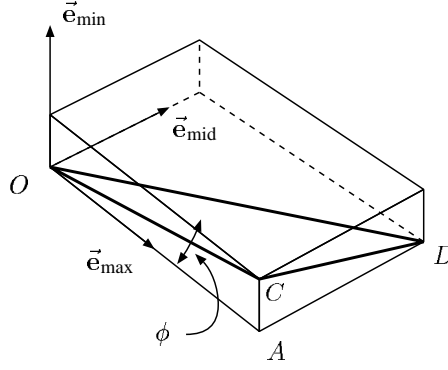


Figure 3.4: The triangle COD is contained in the plane. The MAD_2 value represents the angle of deviation of the regression line \overline{OA} from this plane.

length of the segment \overline{AB} . It is given by

$$\begin{aligned} |\overline{AB}| &= \sqrt{|\overline{AD}|^2 + |\overline{BD}|^2} \\ &= \sqrt{(\sqrt{\lambda_{\text{mid}}})^2 + (\sqrt{\lambda_{\text{min}}})^2} \\ &= \sqrt{\lambda_{\text{mid}} + \lambda_{\text{min}}}. \end{aligned}$$

Therefore, the angle θ can be calculated as

$$\theta = \tan^{-1} \left(\frac{|\overline{AB}|}{|\overline{OA}|} \right) = \tan^{-1} \left(\sqrt{\frac{\lambda_{\text{mid}} + \lambda_{\text{min}}}{\lambda_{\text{max}}}} \right).$$

This is the first MAD value used by Kirschvink. It is usually called MAD_1 .

A second approximation to the maximum angular deviation of the data points from the regression line uses the plane containing the triangle COD in Figure 3.4. The MAD value is the angle ϕ between the plane and the line \overline{OA} . To calculate this, we calculate the vector \vec{OC} and the vector \vec{OD} . These vectors both lie in the plane, and their cross product will produce a vector normal to the plane.

To calculate this normal vector, we write

$$\begin{aligned} \vec{OC} &= \sqrt{\lambda_{\text{max}}} \vec{e}_{\text{max}} + \sqrt{\lambda_{\text{min}}} \vec{e}_{\text{min}} \text{ and} \\ \vec{OD} &= \sqrt{\lambda_{\text{max}}} \vec{e}_{\text{max}} + \sqrt{\lambda_{\text{mid}}} \vec{e}_{\text{mid}}. \end{aligned}$$

Then the normal vector \vec{n} is defined to be

$$\begin{aligned}\vec{n} &= \sqrt{\lambda_{\max}^2}(\vec{e}_{\max} \times \vec{e}_{\max}) + \sqrt{\lambda_{\max}\lambda_{\text{mid}}}(\vec{e}_{\max} \times \vec{e}_{\text{mid}}) + \\ &\quad \sqrt{\lambda_{\min}\lambda_{\max}}(\vec{e}_{\min} \times \vec{e}_{\max}) + \sqrt{\lambda_{\min}\lambda_{\text{mid}}}(\vec{e}_{\min} \times \vec{e}_{\text{mid}}) \\ &= \sqrt{\lambda_{\max}\lambda_{\text{mid}}}\vec{e}_{\min} + \sqrt{\lambda_{\min}\lambda_{\max}}\vec{e}_{\text{mid}} - \sqrt{\lambda_{\min}\lambda_{\text{mid}}}\vec{e}_{\max}.\end{aligned}$$

Since \vec{e}_{\min} , \vec{e}_{mid} , and \vec{e}_{\max} are orthonormal vectors, the angle of deviation of \vec{n} from the plane perpendicular to \vec{e}_{\max} is equivalent to the angle ϕ . The projection of \vec{n} onto the \vec{e}_{\min} axis has length $\sqrt{\lambda_{\max}\lambda_{\text{mid}}}$, the projection of \vec{n} onto the \vec{e}_{mid} axis has length $\sqrt{\lambda_{\max}\lambda_{\min}}$, and the projection of \vec{n} onto the \vec{e}_{\max} axis has length $\sqrt{\lambda_{\text{mid}}\lambda_{\min}}$. By analogy with calculation of MAD₁ the angle ϕ is equal to

$$\begin{aligned}\phi &= \tan^{-1} \left(\sqrt{\frac{\lambda_{\text{mid}}\lambda_{\min} + \lambda_{\max}\lambda_{\min}}{\lambda_{\max}\lambda_{\text{mid}}}} \right) \\ &= \tan^{-1} \left(\sqrt{\frac{\lambda_{\min}}{\lambda_{\max}} + \frac{\lambda_{\min}}{\lambda_{\text{mid}}}} \right).\end{aligned}$$

This is the second MAD value of Kirschvink, denoted MAD₃.

These MAD values are approximations only. Today's computers are substantially faster than those available to earlier researchers and calculating the exact MAD is now possible. Using actual MAD values, we can easily determine the points to include in each analysis and apply an automated routine to find the best fit, as discussed in the following section.

3.2 NRM Visualization

In the past, a paleomagnetic researcher performed the analysis of demagnetization data using a Zijderveld diagram [12] (see Figure 3.5). This method, which dates back to 1967, was developed specifically to display three-dimensional data in two dimensions. In a

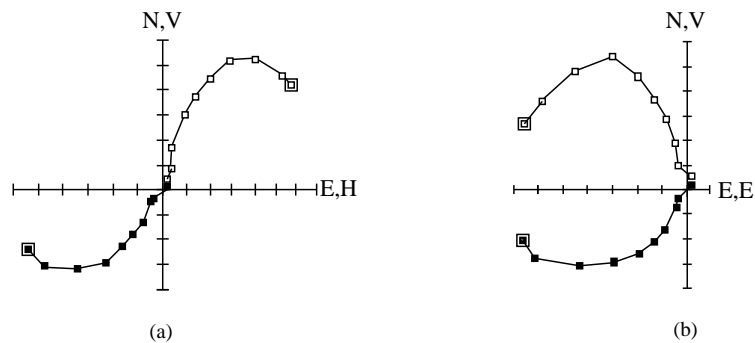


Figure 3.5: Two types of Zijderveld plots. The filled boxes are plotted with respect to the north-south axis and the east-west axis; the unfilled boxes are plotted with respect to the up-down axis and to the total horizontal axis (a), or east-west axis (b).

Zijderveld plot the three-dimensional points are projected onto two orthogonal planes — one that represents the horizontal component and one that represents the vertical component — and are displayed as one plot. In order to adequately view each sample, more than one projection is often required.

However, the data points given by the demagnetization process are three-dimensional. Using a visualization approach, we have improved upon the Zijderveld plot by displaying each demagnetization result as a vector. This type of display, as shown in Figure 3.6, allows real time interaction with the image. The three-dimensional view also allows us to examine the samples from any angle, eliminating the need for a projection onto a plane, and giving a more meaningful representation of the data.

The analysis of each sample is further improved through automation. The conventional analysis technique requires a scientist to utilize a Zijderveld diagram and to manually select the appropriate points to be used in the PCA. However, we have implemented a search routine that looks at many combinations of data points for each sample and finds the best fit for the characteristic NRM (Figure 3.7).

To use a combinational search routine, we first take a set of points and create all

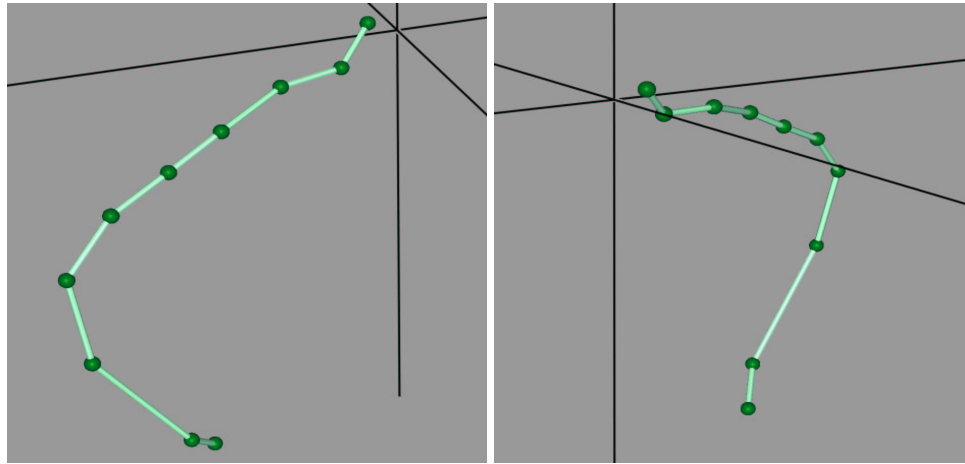


Figure 3.6: Demagnetization plots of the data shown in the previous Zijdeveld plots. The initial points represent the secondary magnetization and are distributed far from the origin. The last few points reflect the characteristic magnetization and are nearly linear approaching the origin. Note how this three-dimensional view gives much more information than the Zijdeveld diagram.

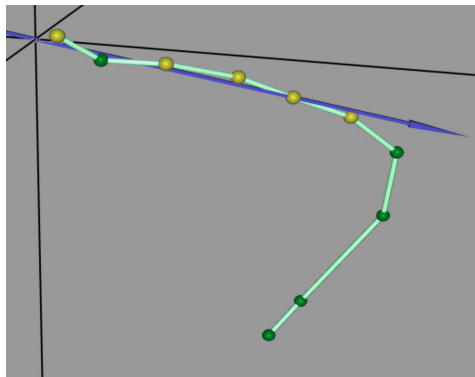


Figure 3.7: Principal component analysis was used to obtain a vector direction for the magnetic field from this sample. The green points represent vector directions of a secondary NRM, while the yellow represents the desired characteristic NRM. In this case, the automated selection algorithm chooses the yellow points to determine the direction, discarding the green values.

combinations of k points out of the n points. The number of possible combinations for a sample is given as:

$$\binom{n}{k} = \frac{n!}{k!(n-k)!}. \quad (3.2)$$

Then, for each combination, we perform a PCA and calculate the MAD. The combination with the lowest MAD is chosen as the best set of points to represent the characteristic NRM.

In order to make this computation as easy as possible, we have included a user interface that allows one to scroll or page through sets of data, making quick and easy comparisons, and doing automatic or manual PCA and MAD calculations (Figure 3.8).

Current Sample
Sample ID: #5-04 ◀ 2 ▶

Input Data

	level	Declination	Inclination	Intensity
<input type="radio"/>	10	45.6	53.9	0.000119
<input type="radio"/>	20	47.9	56	9e-05
<input type="radio"/>	30	43.2	57.9	5.95e-05
<input type="radio"/>	40	41.7	60.8	4.2e-05
<input checked="" type="radio"/>	50	45.4	64.7	3.15e-05
<input type="radio"/>	60	38	68.6	2.48e-05
<input checked="" type="radio"/>	70	48.5	66	2.01e-05
<input checked="" type="radio"/>	80	62.5	68	1.43e-05
<input checked="" type="radio"/>	90	55.9	64.3	1.14e-05
<input checked="" type="radio"/>	100	73.7	66.6	7.97e-06

Pick best fit starting with demag level 40 and use 5 pts Apply

Output Data

Number Of Points: 5

Declination Inclination
49.5344 65.5684

Maximum Angular Deviation:

MAD 9.78822
*MAD1 13.191
*MAD3 3.13061

Views

NE-Proj Data Box Reset View
EV-Proj
NY-Proj
PCA-Proj

Quit

Figure 3.8: User interface for the NRM calculation application. The interface allows one to scroll through the samples using the top set of arrow buttons. The user can manually select specific points to be included in the PCA or specify the number of points to be included and allow the computer to find the best combination of points for an optimal MAD. The bottom set of buttons allows multiple views of data projected onto a plane.

Chapter 4

Collective Data Analysis

Once the data have been collected and measurements have been performed in the laboratory, the history of the magnetic field can be studied by examining successive samples. Many paleomagnetic studies now involve the collection of a sequence of samples from an outcrop or a sediment core. By viewing the changes in successive samples, paleomagnetists can study the changes that take place over time. For example, sediments at the bottom of a sequence of samples were deposited earlier and therefore contain an older record of the earth's magnetic field while sediments at the top of the sequence were deposited more recently and contain a younger record of the magnetic field. This sequence of samples gives a history of the earth's changing magnetic field.

Our visualization approach to this type of data set involves the display of a sequence of directions as arrows arrayed along a core or spine. This approach allows a user to view changes in both the intensity and direction at the same time. An additional visualization technique that we have developed allows a user to view data from two separate sequences, or cores at the same time in order to make correlations between them.

4.1 Time-Sequence Analysis

At the present time, time-sequence analysis is most often done by plotting depth versus inclination, depth versus declination, or depth versus intensity. An example can be seen in Figure 4.1. These plots are used to examine polarity reversals and make correlations between cores (as discussed in Section 4.2).

We have improved upon this technique by displaying all the magnetic components at the same time in sequence. This approach allows a paleomagnetist, for the first time, to examine the history of the magnetic field, with both the intensity and direction of the vectors displayed simultaneously. The data are displayed as shown in Figure 4.2 and Figure 4.3.

One advantage of displaying the data in this way is that it allows a paleomagnetist to view the interrelationship between the changes in direction and the changes in intensity, which cannot be done with two-dimensional plots. The sequence can be displayed in several ways:

- As paleomagnetic vectors, with direction and intensity (Figure 4.2)
- As unit vectors (Figure 4.3)
- As relative vectors where the measured intensity of each sample is normalized by some parameter

In addition to providing a three-dimensional view of the data, the program includes a two-dimensional view (similar to Figure 4.1) that is displayed in the same application. This allows a paleomagnetist to view one component at a time while also examining the entire sequence in three dimensions.

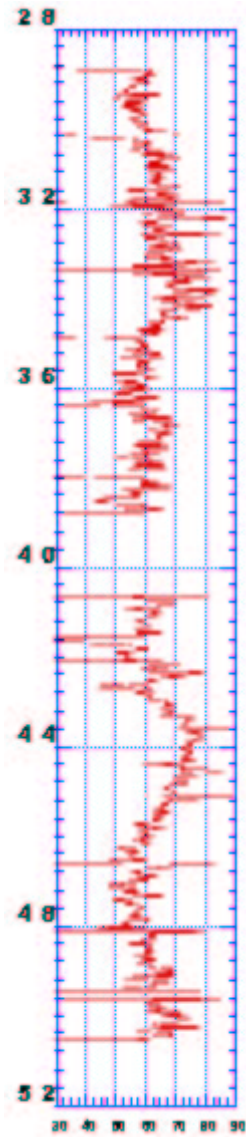


Figure 4.1: Two-dimensional plot of position versus inclination for two cores.

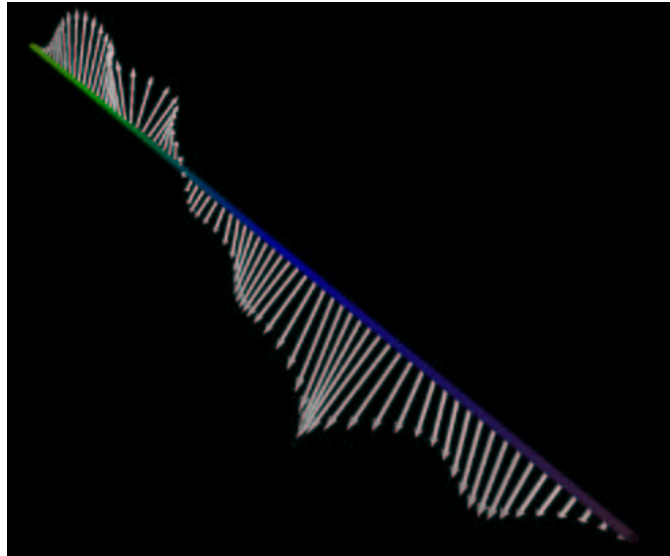


Figure 4.2: A time-sequence display of paleomagnetic data from a section of a sediment core. The image displays the vectors with their intensity. In this section of the core we observe a polarity change in the magnetic field.

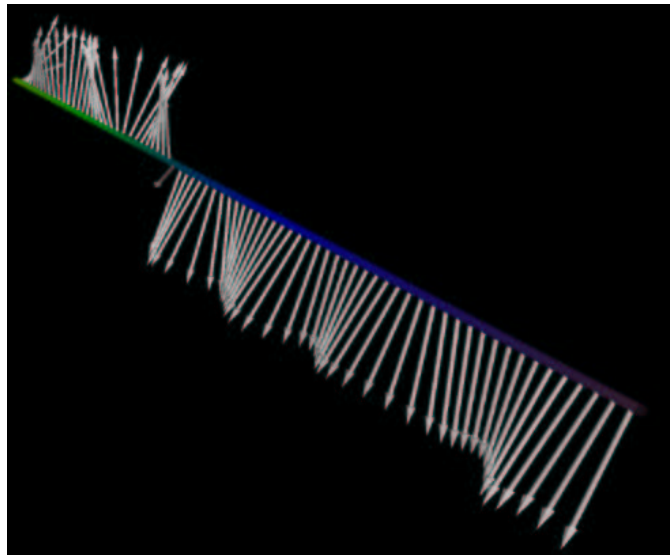


Figure 4.3: The time-sequence display of 4.2 with vectors of constant length.

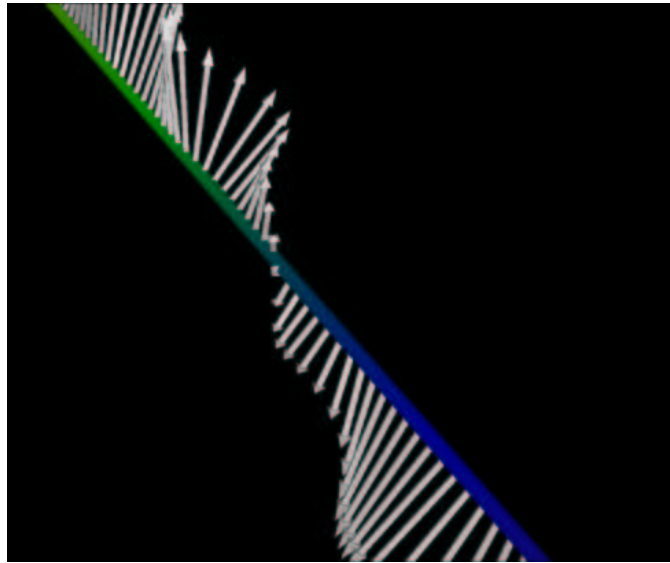


Figure 4.4: Close-up view of the section from 4.2 where the polarity change occurs.

4.2 Core Merging and Analysis

In order to obtain a complete record of the magnetic field, it may be necessary to examine and combine data from sediment cores from one or more sites. The cores taken from each site are often collected without azimuthal orientation. In addition, there may be gaps between cores from a given site. By combining and rotating cores relative to each other, we can align the cores and fill in the gaps.

Previously, this analysis was done using a simple spreadsheet program and two-dimensional plots of depth versus inclination, depth versus declination, or depth versus intensity. The data were adjusted based on these plots so that the completed record could be matched as close as possible. Figure 4.1 shows a gap between two cores that must be filled with another core taken from the same site and at the same depth.

Our visualization approach to this problem provides three-dimensional displays of cores that can be merged together (Figure 4.5). Once two cores have been selected and

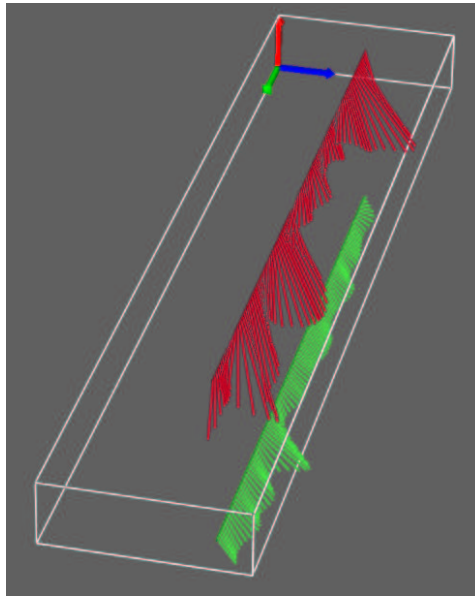


Figure 4.5: Two cores plotted in three dimensions.

displayed on the screen in three-dimensional space, the user can rotate and expand the cores to get the best view of the data. In addition, the user has the option of changing the position and declination of each core.

Chapter 5

Virtual Geomagnetic Poles

The directions and magnitude of the geomagnetic field of the earth change with time. Paleomagnetists use virtual geomagnetic poles (VGPs) to view these changes. VGPs are pole positions calculated from a single observation of the direction of the geomagnetic field. Combinations of these pole positions provide a history of the changes with respect to a designated location. The two uses of VGPs — viewing polarity transitions and studying paleosecular variation, are described in the sections below.

5.1 Polarity Transitions

Polarity transitions are large-scale changes in the earth's magnetic field. The normal polarity state of the geomagnetic field is characterized by declinations that point northward and inclinations that point downward in the northern hemisphere and upward in the southern hemisphere. The opposite of this is a reversed polarity state. This mysterious change from one polarity state to the other takes place infrequently — anywhere from 50,000 years to many millions of years. The Magnetic Polarity Time Scale documents the normal

and reversed states over the past 200 million years. Polarity changes, or large-scale secular variations, in the magnetic field cannot be easily viewed in two dimensions, as they extend beyond a single hemisphere.

Currently, the best way to view data from a polarity transition is with a stereographic projection onto a circle that represents the earth, or with a simple Cartesian plot (Figure 5.1). Both methods fail to fully represent the true vector nature of the data.

Using three-dimensional analysis techniques, we display polarity transition data on a sphere (Figure 5.2). By projecting a set of data onto the unit sphere and using a curve to connect the points on the sphere, we can view the pole position as it undergoes a complete reversal. The user can view data that wraps around the sphere by rotating the sphere or making the sphere transparent.

5.2 Paleosecular Variation on a Sphere

Changes in direction on a smaller scale, are called *geomagnetic secular variation*. The most common way to examine these data involves a stereographic projection (see [1]) onto a plane (as in Figure 5.3). With this approach, only a limited portion of the curve can be displayed.

Using three-dimensional analysis techniques, we draw the data directly on the sphere, eliminating the need for two-dimensional projections. In addition, we present secular variation from a common origin as a “movie” to facilitate examination of the changes in intensity, as shown in Section 5.3.

Figure 5.4 is an example of a secular variation curve showing changes in declination and inclination over time. In this way, a paleomagnetist can view the entire sphere instead

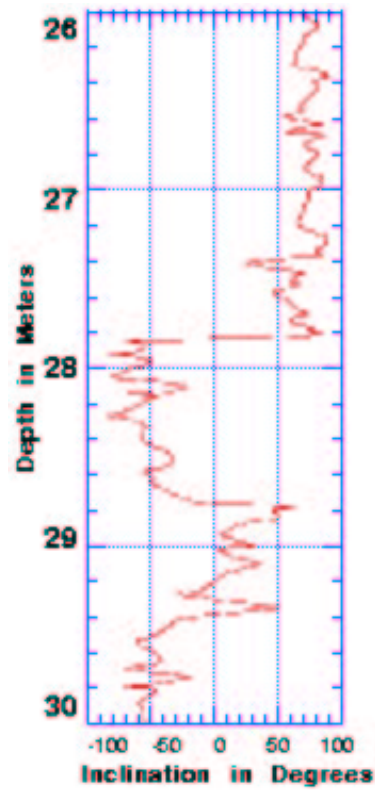


Figure 5.1: Two-dimensional plot of a polarity transition. A transition from positive to negative inclination indicates a polarity reversal.

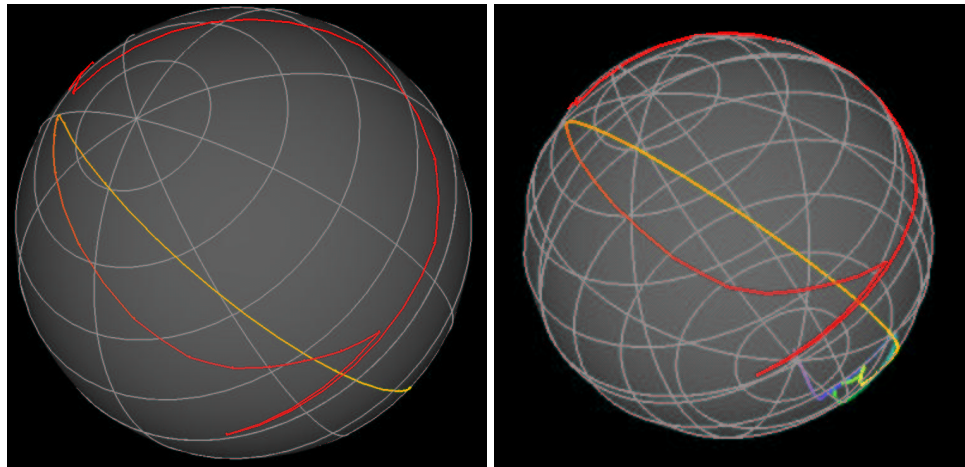


Figure 5.2: Two views of a polarity transition plotted on a sphere. The image on the right shows a transparent view that allows us to examine data on the other side of the sphere (or globe) without rotating it.

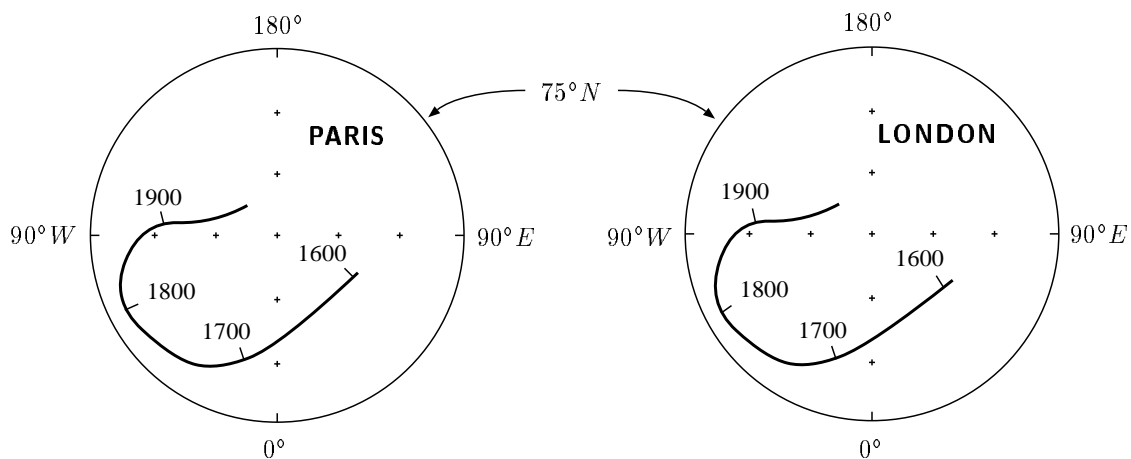


Figure 5.3: Stereographic projection of virtual geomagnetic poles corresponding to secular variation in Paris and London for the past 400 years.

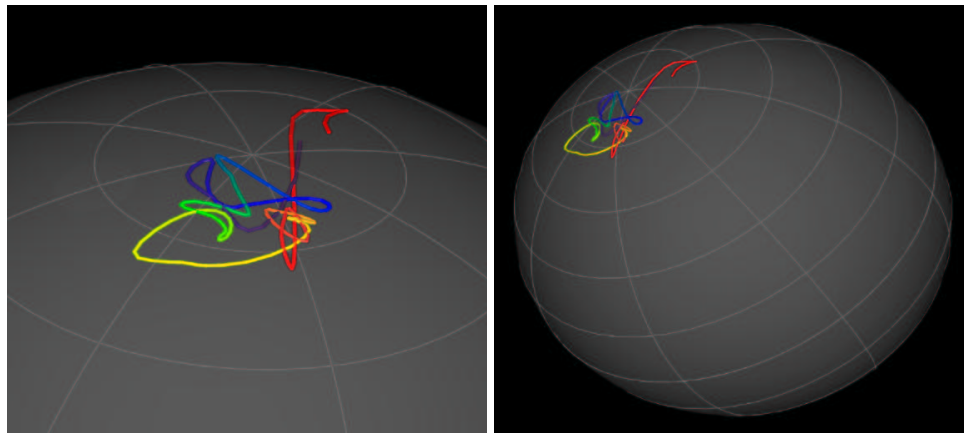


Figure 5.4: Secular variation displayed on a globe. The data is interpolated using a spherical Catmull-Rom curve.

of a two-dimensional projection. Also, the sphere can appear transparent, so the curve can be viewed from any direction.

5.3 Paleosecular Variation Plotted with a Common Origin

Our visualization approaches also provide more flexibility in the analysis of paleomagnetic data sets. In particular, we examine local changes in the magnetic field by representing the field vectors from a single point with a curve [2] drawn through the tips of

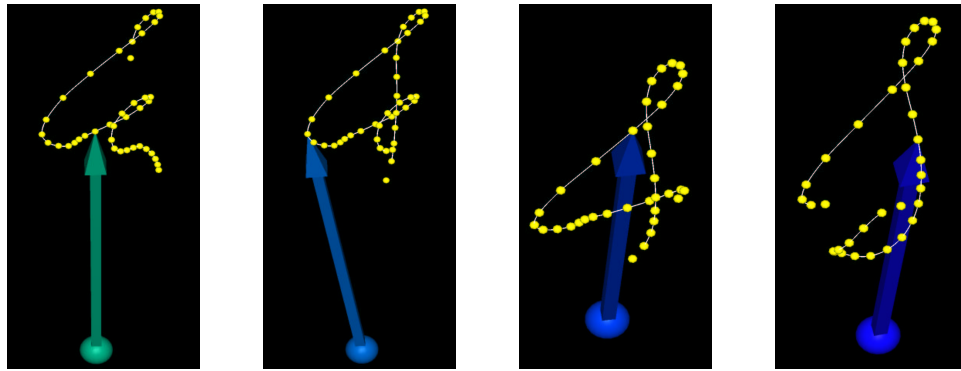


Figure 5.5: Display of local trends using data from Figure 5.4. This sequence of images shows the change in intensity and direction of the vector as it moves along a portion of the curve.

the vectors on either side of a chosen base vector. A paleomagnetist can change the base vector and the length of the curve, thereby obtaining a new representation of the data. Figure 5.5 shows a single screen shot of this movement for successive base vectors. As the base vector moves along the core its length and color change to indicate the intensity of the vector and its position in time along the core, respectively. This application allows us to look at local trends in the magnetic field and to correlate changes in intensity and direction in detail, which was not possible before.

Chapter 6

Demagnetization Profiles

Another way of studying the history of the magnetic field involves examining demagnetization profiles. As a sample is progressively demagnetized, to determine the characteristic NRM, the intensity decreases. A demagnetization profile presents these trends by plotting the intensity at each demagnetization level as a function of position along the core. An example of a demagnetization plotted in two-dimensions is shown in Figure 6.1. By using a visualization approach, we are able to portray more closely and accurately the demagnetization behavior in each section of a core.

We have developed three ways of viewing demagnetization data. The first picture, on the left in Figure 6.2, shows the sample intensity for each level of demagnetization. The peaks represent samples with high intensity, meaning these samples contained relatively large amounts of magnetic grains.

The second picture, shown on the right in Figure 6.2, depicts the data after they have been normalized by the initial magnetization. By normalizing the data, we can view directly the downcore variations in coercivity.

The third method (Figure 6.3) shows the rate of change in intensity for each sample

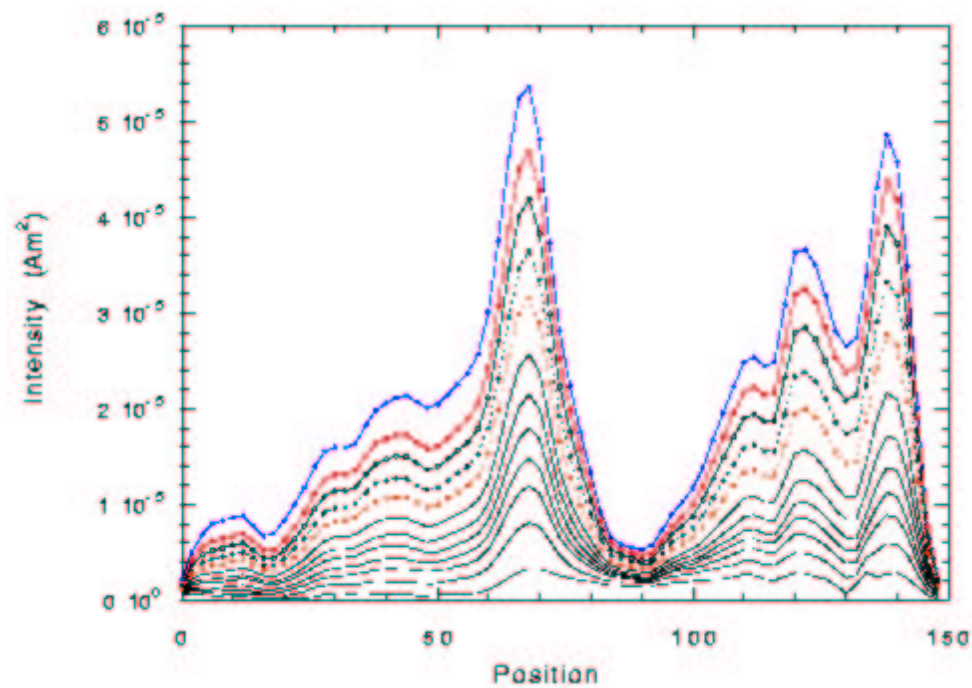


Figure 6.1: Two-dimensional plot of position versus intensity. Each curve indicates the demagnetization level at which each sample was measured.

during progressive demagnetization. This image demonstrates the difficulty associated with the removal of the secondary magnetization.

Demagnetization profiles are used to study climatic history. By examining these plots, paleomagnetists can determine past climate change. These profiles also indicate changes in sediment source. By looking at the change in the proportion of different components of the sediment, paleomagnetists can, for example, determine when a mud slide occurred or where a river pattern changed.

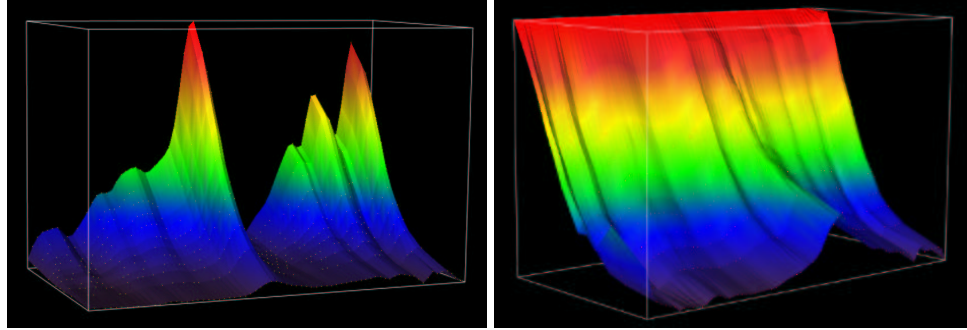


Figure 6.2: Two demagnetization profiles. The image on the left shows the coercivity data resulting from multiple demagnetizations. The image on the right shows the same data normalized by the original intensity magnetic value.

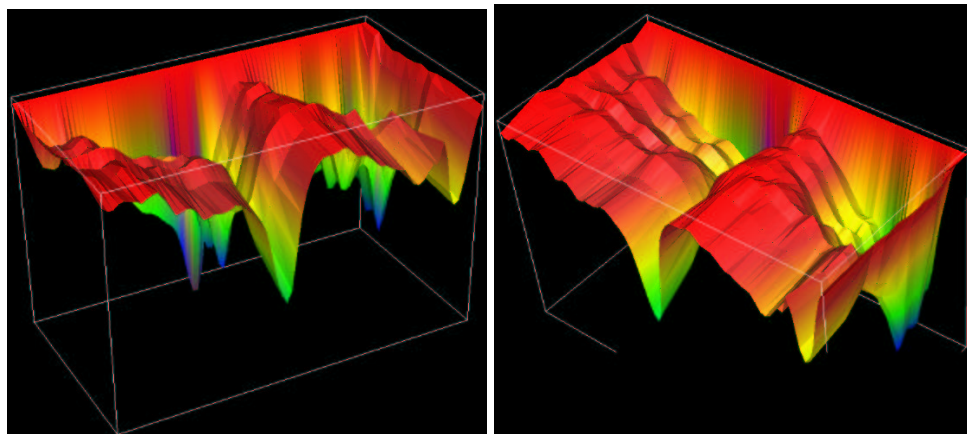


Figure 6.3: Two views showing the rate of change that takes place within each sample.

Chapter 7

Conclusions

Paleomagnetists have been representing data using the same methods for over 40 years. These representation techniques reflect the fact that the collection and measurement of data was the time-consuming portion of the collection-measurement-analysis process. With new automated collection techniques and in-line measurement devices, the rate at which samples can be measured now exceeds the rate at which data can be analyzed by these methods.

Current data analysis techniques in paleomagnetism are based on projections of three-dimensional data onto two-dimensional planes as seen in Zijderveld diagrams and stereographic projections. In many cases this requires several projections in order to examine even a small set of data. In addition, current numerical analysis techniques introduced by Kirschvink estimate values rather than compute the exact values of certain parameters. Finally, many of these techniques only permit the analysis of one sample at a time or views of one component at a time.

Using visualization approaches, we have developed a suite of tools that give a paleomagnetist new and better ways of analyzing data. These tools permit faster and more

accurate analysis of individual samples. We also implement a user interface that allows for analysis of large data sets. By representing data in three dimensions, we have introduced new ways to visually analyze data and view it in three-dimensions. By introducing these new ways of visualizing paleomagnetic data, we have opened up areas of research not previously possible due to the limitations of two-dimensional representations. These methods give paleomagnetists more information and a more realistic representation of the geomagnetic field along with new tools for its analysis.

7.1 Implementation

All computer programs were developed at the Center for Image Processing and Integrated Computing at the University of California, Davis. These applications were created and tested on a Silicon Graphics O2 platform running Irix 6.3. The user interface, which allows the user to interact with the program, is implemented with Xforms and all the graphics routines are programmed using OpenGL. All other code is written in object oriented C++. Data is read into each program from an ASCII text file. The images in all applications are interactive and allow one to rotate and view data from different angles in real time.

Bibliography

- [1] Robert F. Butler. *Paleomagnetism: Magnetic Domains to Geologic Terranes*. Blackwell Scientific Publications, Boston, MA, 1992.
- [2] Edwin Catmull and Raphael Rom. A class of local interpolating splines. In Robert E. Barnhill and Richard F. Riesenfeld, editors, *Computer Aided Geometric Design*, pages 317–326. Academic Press, 1974.
- [3] G. H. Golub and C. F. Van Loan. *Matrix Computations*, 2nd ed. Johns Hopkins University Press, Baltimore, 1989.
- [4] E. Jurrus, K. Verosub, and K. Joy. Computer graphics methods for the display and analysis of large paleomagnetic datasets. In *1998 Spring Meeting*, volume 17, page F224. American Geophysical Union, Eos, Transactions, May 1998.
- [5] E. Jurrus, K. Verosub, K. Joy, and J. Stoner. Interactive computer graphics methods for the display and analysis of large paleomagnetic datasets. In *1998 Fall Meeting*, volume 79, page S73. American Geophysical Union, Eos, Transactions, December 1998.
- [6] J. L. Kirschvink. The least-squares line and plane and the analysis of paleomagnetic data. *Geophysical Journal of the Royal Astronomical Society*, 62:699–718, 1980.

- [7] Ken Shoemake. Animation rotations with quaternion curves. *Computer Graphics*, 19(3):245–254, 1985.
- [8] Ken Shoemake. Arcball rotation control. In Paul Heckbert, editor, *Graphics Gems IV*, pages 175–192. Academic Press, Boston, 1994.
- [9] Kenneth L. Verosub. Depositional and post-depositional processes in the magnetization of sediments. *Review of Geophysics and Space Physics*, 15:129–143, 1977.
- [10] Kenneth L. Verosub and A.P. Roberts. Environmental magnetism: Past, present and future. *Journal of Geophysical Research*, 100:2175–2192, 1995.
- [11] R.J. Weeks, C. Laj, L. Endignoux, M.D. Fuller, A.P. Roberts, R. Manganne, E. Blanchard, and W. Goree. Improvements in long core measurement techniques: applications in palaeomagnetism and palaeoceanography. *International Journal of Geophysics*, 114:651–662, 1993.
- [12] J.D.A. Zijdeveld. A.C. demagnetization of rocks: Analysis of results. In D.W. Collinson, K.M. Creer, and S.K. Runcorn, editors, *Methods in Palaeomagnetism*, pages 254–286. Elsevier Publishers, Amsterdam, Boston, 1967.